Supplemental Document

Biomedical Optics EXPRESS

Laser pulse train parameters determine the brightness of a two-photon stimulus: supplement

Marcin J. Marzejon,[1,2,3] Łukasz Kornaszewski,[1,2] Maciej Wojtkowski,[1,2] and Katarzyna Komar[1,2,4,*]

[1] *International Centre for Translational Eye Research, Skierniewicka 10a, 01-230 Warsaw, Poland*
[2] *Department of Physical Chemistry of Biological Systems, Institute of Physical Chemistry, Polish Academy of Sciences, M. Kasprzaka 44/52, 01-224 Warsaw, Poland*
[3] *Department of Metrology and Optoelectronics, Faculty of Electronics, Telecommunications and Informatics, Gdańsk University of Technology, G. Narutowicza 11/12, 80-233 Gdańsk, Poland*
[4] *Institute of Physics, Faculty of Physics, Astronomy and Informatics, Nicolaus Copernicus University in Torun, Grudziądzka 5, 87-100 Toruń, Poland*
[*] *kkomar@fizyka.umk.pl*

Supplement DOI: https://doi.org/10.6084/m9.figshare.22717117

Parent Article DOI: https://doi.org/10.1364/BOE.489890

Laser pulse train parameters determine the brightness of a two-photon stimulus

MARCIN J MARZEJON,[1–3] ŁUKASZ KORNASZEWSKI,[1,2] MACIEJ WOJTKOWSKI,[1,2] AND KATARZYNA KOMAR[1,2,4*]

[1]*International Centre for Translational Eye Research, Skierniewicka 10a, 01-230 Warsaw, Poland*
[2]*Department of Physical Chemistry of Biological Systems, Institute of Physical Chemistry, Polish Academy of Sciences, M. Kasprzaka 44/52, 01-224 Warsaw, Poland*
[3]*Department of Metrology and Optoelectronics, Faculty of Electronics, Telecommunications and Informatics, Gdańsk University of Technology, G. Narutowicza 11/12, 80-233 Gdańsk, Poland*
[4]*Institute of Physics, Faculty of Physics, Astronomy and Informatics, Nicolaus Copernicus University in Torun, Grudziądzka 5, 87-100 Toruń, Poland*
**kkomar@fizyka.umk.pl*

S1. Pulse train parameter measurements

For each obtained pulse train, the pulse duration and spectrum measurements were performed. The pulse duration was obtained based on an intensity autocorrelation measurement using a commercial autocorrelator (PulseCheck, APE). Only for the 750 ps-long pulse, a fast InGaAs photodiode (1414, NewFocus, 3 dB bandwidth 25 GHz, rise time 14 ps) and a fast oscilloscope (SDA 760Zi-A, Teledyne Lecroy, 6 GHz bandwidth) were employed. The autocorrelation measurements with sech^2 (for solid-state sub-picosecond laser; *fs laser* and spectrally-shifted frequency-doubled femtosecond Er-doped fiber laser; *tunable fs laser*) or Gaussian fit (fiber-optics picosecond laser; *ps laser*) are presented in Fig. S1. The shape of the fitting curve was provided by the laser manufacturer.

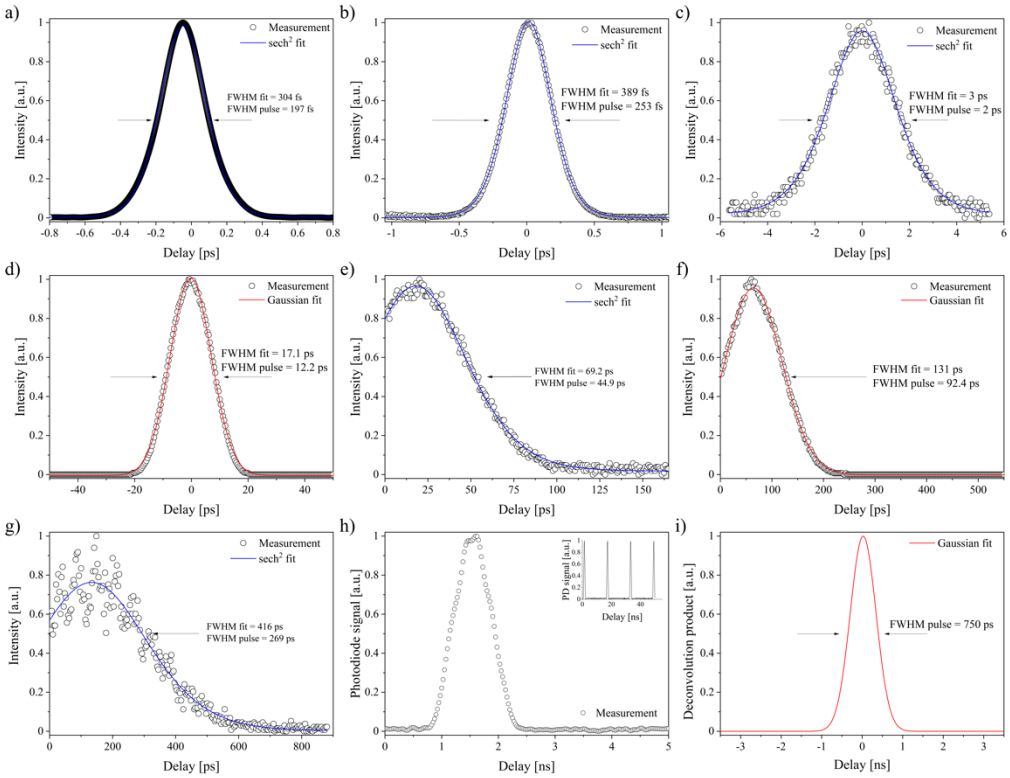

Fig. S1. Determination of pulse duration of various pulse trains used in the experiments. Intensity autocorrelation curves for pulses from: a) spectrally-shifted frequency-doubled femtosecond Er-doped fiber laser (*tunable fs laser*), b) solid-state sub-picosecond laser (*fs laser*), c) *fs laser* stretched with a grating-based stretcher, d) fiber-optics picosecond laser (*ps laser*), e) *fs laser* stretched with a fiber-based stretcher (100 m), f) *ps laser* stretched with a fiber-based stretcher (1 km), g) *fs laser* stretched with a fiber-based stretcher (100 m), with the corresponding fit function. h) Photodiode signal registered for *fs laser* pulses stretched with a fiber-based stretcher (1 km). i) Deconvolution result originated from waveform registered by a fast photodiode (h) assuming a Gaussian pulse shape. Abbreviations: FWHM – full width at half maximum, PD – photodiode. All plots are normalized to 1.

The results presented in the Fig. S1 need a few comments. First of all, with the employed autocorrelator, the autocorrelation function is measured only for half of the delay range when it is longer than 300 ps. This approach is reasonable as the autocorrelation function is symmetrical [1]. Secondly, it can be observed that the quality of the fit is associated with the

intensity of the second harmonic signal generated at the crystal in the autocorrelator. Therefore, for the longest pulses the quality of fit decreases with lower peak power and the second harmonic generation efficiency (compare Fig. S1 a) and g)).

For the 750 ps pulses, the actual functional shape of the fit curve may be subject to an error. Notably, after passing through 1 km of an optical fiber, the shape of the pulse may be distorted due to the extensive amount of dispersion. The coefficient of determination, which reflects the quality of fit of the model to the data, was higher for Gaussian fit (0.997) than for $sech^2$ fit (0.994) and therefore applied. This approach is reasonable as the quality of data fit determines the quality of the determination of full width at half maximum pulse duration.

The differences between pulse duration of various pulse trains are visualized in Fig. S2. The longest pulse used in the psychophysical experiments is above three orders of magnitude longer than the shortest one.

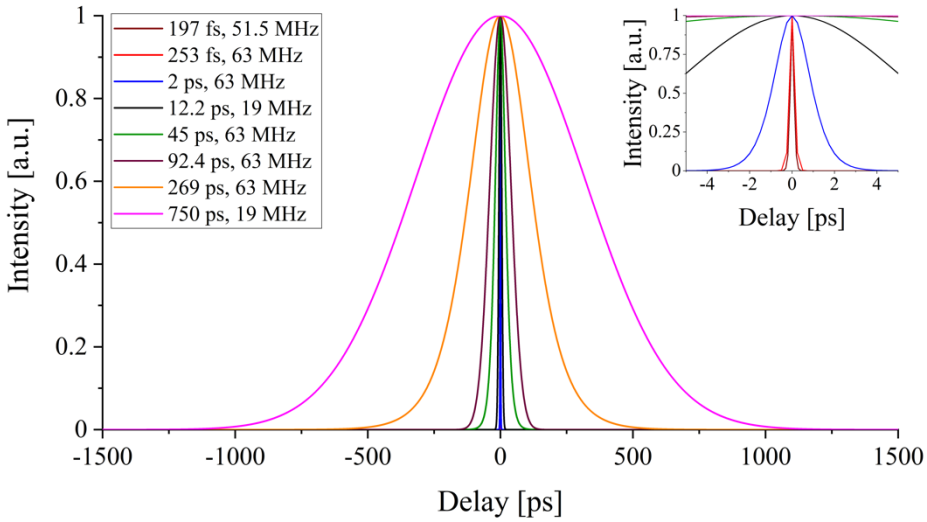

Fig. S2. The comparison of pulse durations for various pulse trains used in the experiments. As over 3 orders of magnitude difference between the shortest and the longest pulse, the 197 fs and 253 fs pulses are visible only in the inset.

An optical spectrum analyzer (AQ-6315E, Ando) was employed to measure the spectral properties of the pulse trains used in the experiments. The acquired spectra are shown in the Fig. S3. All three lasers used in the experiments vary in terms of the central wavelength and the spectral width. However, the spectral parameters of *tunable fs laser* and *fs laser* are very similar.

For all pulses stretched using the fiber-based stretcher, the nonlinear effect of self-phase modulation is probably responsible for the spectral broadening of the pulse [2]. Different amount of spectral broadening for each case results from an interplay of dispersion and nonlinearities in the stretching fiber (also dependent on coupling efficiency, which directly translates to a peak power of the pulse propagating in the fiber).

For the pulses originated from *fs laser*, the central wavelength remained the same (1043.3 nm) for each pulse duration and despite of the stretcher. In general, the spectral bandwidth increases with the pulse duration. Only for 45 ps pulses, the broadening is significantly higher than for 269 ps pulses originated from the same laser. This fact may be explained by the differences in the length of the optical fiber (100 m for 45 ps and 1 km for 269 ps pulses) and the optical power density level at the fiber input. In the case of *ps laser*, the measured spectrum of a stretched pulse is altered. However, the spectral bandwidth defined as full-width at tenth-maximum remains the same (26.9 nm). The central wavelength is slightly shifted and equal to 1029.3 nm.

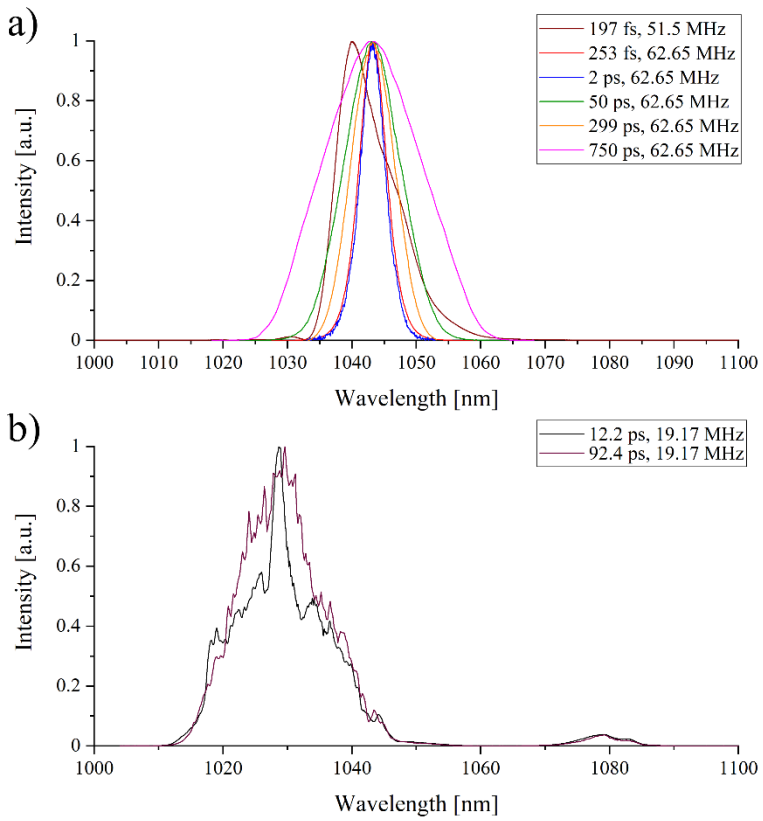

Fig. S3. Spectral properties of laser pulse trains originated from: a) *tunable fs laser* and *fs laser*, b) *ps laser.* All plots are normalized to 1.

S2. Safety considerations for psychophysical experiments

To maintain a safe eye illumination during psychophysical experiments, we followed the ANSI Z136.1:2014 [3] guides to calculate the maximum permissible exposure for the experiment. As mentioned in the Section 2.2, we assumed a 5 minutes-long exposure for a stationary beam as during the psychophysical experiments a single retinal spot is illuminated for a much shorter time due to: (1) flickering stimulus; (2) ring stimulus instead of a stationary beam; (3) various retinal locations investigated during the test; and (4) the 5- 7 minutes' examination time.

ANSI Z136.1:2014 specifies three Rules that apply for pulsed near-infrared radiation entering the eye. For the high repetition rate pulse trains, the most restrictive is the Rule 2. Table S1 summarizes the maximum permissible exposure levels calculated for Rules 1-3, assuming a 7 mm pupil diameter. For most of the pulse trains, 400 μW safety limit was set as the safety limit and the highest possible power level of the beam at the pupil plane. This value corresponds to an 1 hour exposure to a stationary beam as showed in [4]. However, for the longest pulse duration of 759 ps, the exposure limit has been elevated to 800 μW. Note that for the considered pulse trains, each safety limit level is below the maximum average radiant power specified in ANSI standard.

Table S1. Calculated safety levels for 5 minutes' exposure of each pulse train used in the presented experiments. Descriptions: τ – pulse duration at full width at half maximum, PRF – pulse repetition frequency, $MP\Phi_i$ – MPΦ level corresponding to Rule i, MPΦ – Maximum Permissible Radiant Power. Safety limit is the safety limit applied during the experiment based on MPΦ analysis.

τ	PRF [MHz]	$MP\Phi_1$ [kW]	$MP\Phi_2$ [μW]	$MP\Phi_3$ [mW]	MPΦ [μW]	Safety limit [μW]
197 fs	51.50	195.43	805	5.62	805	400
253 fs	62.65	152.17	808	6.51	808	400
2 ps	62.65	19.25	808	6.51	808	400
12.2 ps	19.17	28.58	754	24.28	754	400
44.9 ps	62.65	8.32	808	63.23	808	400
92.4 ps	19.17	3.79	758	24.39	758	400
269 ps	62.65	1.39	808	63.23	808	400
759 ps	62.65	0.49	808	63.23	808	800

References

1. J.-C. Diels and W. Rudolph, "Fundamentals," in *Ultrashort Laser Pulse Phenomena - Fundamentals, Techniques, and Applications on a Femtosecond Time Scale*, J.-C. Diels and W. Rudolph, eds., 2. (Academic Press, 2006), p. 5.
2. G. Agrawal, *Nonlinear Fiber Optics*, 5th ed. (Academic Press, 2012).
3. American National Standard Institute, *American National Standard for Safe Use of Lasers (ANSI Z136.1-2014)* (2014).
4. M. J. Marzejon, Ł. Kornaszewski, J. Bogusławski, P. Ciąćka, M. Martynow, G. Palczewska, S. Maćkowski, K. Palczewski, M. Wojtkowski, and K. Komar, "Two-photon microperimetry with picosecond pulses," Biomed. Opt. Express **12**(1), 462–479 (2021).

S3. The influence of the pulse shape on the two-photon visual threshold.

As shown in Section 2.3, the two-photon visual threshold power level P_{2phVT} depends, among others, on the pulse shape:

$$P_{2phVT} = a \cdot \sqrt{\delta} \cdot \frac{F}{\sqrt{E}} \tag{S1}$$

where a is a coefficient that has a physical interpretation of a material constant of the retina that combines the visual threshold value expressed as mean power value with the pulse train parameters, δ is the duty cycle, and E and F are terms related to the pulse shape (see Equations 13, 14, 17, and 18):

$$E_{gaussian} = \frac{1}{2} \cdot \sqrt{\frac{\pi}{\ln 4}} \cdot \mathrm{erf}\left(\frac{4 \ln 4}{\delta}\right), \tag{S2}$$

$$F_{gaussian} = \frac{1}{2} \cdot \sqrt{\frac{\pi}{\ln 2}} \cdot \mathrm{erf}\left(\frac{4 \ln 2}{\delta}\right), \tag{S3}$$

$$E_{\mathrm{sech}^2} = -\frac{2}{3 \cdot 1.76} \cdot \tanh\left(\frac{3.52}{\delta}\right)\left[\tanh^2\left(\frac{3.52}{\delta}\right) - 3\right], \tag{S4}$$

and

$$F_{\mathrm{sech}^2} = \frac{2}{1.76} \cdot \tanh\left(\frac{3.52}{\delta}\right), \tag{S5}$$

where erf is an error function, and the subscripts gaussian and sech^2 refer to the shape of the pulse. One may wonder how significantly the pulse shape influences the visual threshold or, in other words, how terms E and F may contribute to the visual threshold value. Therefore, we present the analysis of the contribution of those two factors, depending on the pulse shape.

First, let us notice that the duty cycle values are in the range $\langle 0,1\rangle$. Secondly, the value of each term change as a reciprocal of the duty cycle δ. Considering gaussian pulse (Equations S2 and S3): (1) the value of the term $E_{gaussian}$ changes as:

$$E_{gaussian} \sim \mathrm{erf}\left(\frac{4 \ln 4}{\delta}\right), \tag{S6}$$

and (2) the value of the term $F_{gaussian}$ changes as:

$$F_{gaussian} \sim \mathrm{erf}\left(\frac{4 \ln 2}{\delta}\right). \tag{S7}$$

To evaluate the value of those term, let us check their values for the extreme values within the duty cycle range. For the duty cycle value tending towards zero, the value for both terms tends towards the value of err(∞) = 1. On the other hand, for the duty cycle value of 1, the terms denoted as S6 and S7 equals to 0.9999 and 1, respectively (the numbers has been rounded to the fourth significant digit after decimal separator).

For hyperbolic secant squared pulse sech^2 (Equations S4 and S5): (1) the value of the term E_{sech^2} changes as:

$$E_{\mathrm{sech}^2} \sim \tanh\left(\frac{3.52}{\delta}\right)\left[\tanh^2\left(\frac{3.52}{\delta}\right) - 3\right], \tag{S8}$$

and (2) the value of the term F_{sech^2} changes as:

$$F_{\mathrm{sech}^2} \sim \tanh\left(\frac{3.52}{\delta}\right). \tag{S9}$$

Similarly for the gaussian pulse, for the duty cycle value tending towards zero, the value of the hyperbolic tangent term tends towards tanh(∞) = 1. This gives values of –2 and 1 for terms denoted as S8 and S9. On the other hand, for the duty cycle of 1, terms S8 and S9 takes values of -2 and 0.9982, respectively.

Based on the calculated values, the influence of the values of the terms E and F may be summarized as presented in Table S2. Similarly, the influence of those terms for the expected mean power ration *R* (see Equation 16 in Section 2.3) may be evaluated as presented in Table S3. The exact values of *E* and *F* constants for the pulse trains used in the experiments described in this article are presented in Table S4.

Table S2. The influence of the pulse shape on the two-photon visual threshold value. Description: δ – duty cycle, *E*, *F* – terms related to the pulse shape (see Equations S2-S5). The calculated values have been rounded to the fourth significant digit after decimal separator.

Pulse shape	δ	*E*	*F*	$F/\sqrt{\mathrm{E}}$
gaussian	0^+	0.7527	1.0645	1.2269
gaussian	1	0.7526	1.0645	1.2270
sech^2	0^+	0.7576	1.1364	1.3056
sech^2	1	0.7576	1.1343	1.3032

Table S3. The influence of the expected mean power ration *R*. Description: δ – duty cycle, E_i, F_i – terms related to the pulse shape (see Equations S2-S5), *i* -describes the pulse shape (either gaussian or sech^2). The calculated values have been rounded to the fourth significant digit after decimal separator.

Pulse shape		δ	$\sqrt{E_2/E_1}$	F_1/F_2	$\sqrt{E_2/E_1}\cdot(F_1/F_2)$
1	2				
gaussian	gaussian	0^+	1	1	1
gaussian	gaussian	1	1	1	1
gaussian	sech^2	0^+	1.0032	0.9367	0.9398
gaussian	sech^2	1	1.0033	0.9384	0.9415
sech^2	gaussian	0^+	0.9968	1.0675	1.0641
sech^2	gaussian	1	0.9967	1.0656	1.0621
sech^2	sech^2	0^+	1	1	1
sech^2	sech^2	1	1	1	1

Table S4. The influence of the pulse shape on the two-photon visual threshold value. Description: , τ – pulse duration at full width at half maximum, *PRF* – pulse repetition frequency, δ – duty cycle, *E, F* – terms related to the pulse shape (see Equations S2-S5). The calculated values have been rounded to the fourth significant digit after decimal separator.

Laser source	τ [ps]	*PRF* [MHz]	δ	*E*	*F*	$F/\sqrt{E}$
tunable fs laser	0.197	52	1.01×10^{-5}	0.7576	1.1364	1.3056
fs laser	0.253	63	1.58×10^{-5}	0.7576	1.1364	1.3056
fs laser	2	63	1.25×10^{-4}	0.7576	1.1364	1.3056
ps laser	12.2	19	2.34×10^{-4}	0.7527	1.0645	1.2269
fs laser	44.9	63	2.81×10^{-3}	0.7527	1.0645	1.2269
ps laser	92.4	19	1.77×10^{-3}	0.7576	1.1364	1.3056
fs laser	269	63	1.69×10^{-2}	0.7576	1.1364	1.3056
fs laser	759	63	4.70×10^{-2}	0.7576	1.1364	1.3056